U.S. DEPARTMENT OF THE INTERIOR
U.S. GEOLOGICAL SURVEY

TO ACCOMPANY MAP I-2586

MAPPING TIME-DEPENDENT CHANGES IN SOIL-SLIP–DEBRIS-FLOW PROBABILITY

By Russell H. Campbell, Richard L. Bernknopf, and David R. Soller

INTRODUCTION

Risk of personal injury or property damage from rainfall-triggered debris-flow events can be expressed in terms of expected losses if the probability that a potentially hazardous event will occur can be combined with economic data about the value of property and infrastructure that could be lost from such an event. A realistic forecast of expected losses could provide an economic basis for community choices about whether, when, and how to impose regulations for mitigation (such as grading or land use constraints) and assign responsibilities for warning and hazard response. Experience in some landslide-prone communities where grading codes require preconstruction site studies has demonstrated that sufficiently detailed geotechnical studies can provide site-specific deterministic assessments of risks that can be reduced through mitigation (see, for example, Slosson and Krohn, 1982). However, because detailed site studies are relatively costly, geotechnical studies are not commonly made at sites where no significant financial commitment has already been made. Cost also commonly prohibits application of those methods to the kinds of regional assessments that are needed to support responsible decisions for community action.

To be timely, regional risk assessments should take advantage of earth-science data (especially topographic, geologic, and soils maps) that already exist or can be acquired rapidly by reconnaissance techniques. To the extent that the elements of the map data are analogous to variables in established geotechnical models, their relations are expected to parallel those in the models; yet the use of existing regional map data and rainfall records from scattered gaging localities introduces greater uncertainty about spatial and temporal variations in earth materials and rainfall than is normally applied in geotechnical analyses of stability. Probability offers a means to characterize that uncertainty quantitatively. A map sequence that displays changes in the spatial distribution of probabilities provides a way to identify the areas of greatest hazard potential and a visual way to evaluate their relations to topographic or cultural features that may be in harms way.

It has been a fairly common practice for regional data to be synthesized into qualitative susceptibility maps delineating, for example, map units of high, moderate, and low potential for hazard. The qualitative maps can be used by skilled professional planners to guide decisions about land use regulation. However, they cannot be applied directly to a quantitative economic assessment of risk, and maps made by different individuals and agencies for different areas may not be comparable even in a qualitative sense. Probability maps, which can be prepared by using rigorously constrained procedures, address the quantification of uncertainty in space and time and have the potential for comparing hazard levels in different map areas. Probability maps also offer the potential for applying economic analyses (Bernknopf and others, 1988; Bernknopf and others, 1993, p. 4–6) to regulatory decisions at the community or county level about, for example, whether to implement grading requirements for design and construction that will minimize potential landslide hazards, or about when to issue warnings and where to recommend evacuation.

As part of a multidisciplinary study to develop a method to estimate the spatial distribution of different levels of risk from rainfall-triggered debris flows, we used preexisting site studies of debris flows to provide input variables (duration data) for regression on the (time-dependent) survival function of a parametric probability distribution. The regression data base was assembled from published studies of the disastrous effects of the January 3–5, 1982, storm in the San Francisco Bay region, collected chiefly in Ellen and Wieczorek (1988). These studies (1) reported observations of failure times, rainfall rate and duration, and geotechnical characteristics at failure sites, (2) provided maps showing a comprehensive inventory of failures that occurred during the storm, and (3) reported results of scientific studies of geotechnical models and rainfall time-histories related to debris-flow initiation. The parameters determined by the regression were then applied, with variables derived from regional map data for a preliminary study area, to estimate the hazard function probability (of the same parametric distribution), that one or more debris flows will be initiated in a 100-m × 100-m area (a 100-m cell) after a specified duration of heavy rainfall. The calculations were made in a geographic information system (GIS), which provides a means for rapid map display of the spatial distribution of probabilities at different times during a storm, and a series of maps depicting a reconstruction of the January 3–5, 1982, storm was prepared.

This is a progress report addressing only those cells where debris flows might be expected to originate from rainfall-triggered soil slips. Forecasting the probability that rainfall will initiate a soil-slip–debris-flow event in a cell after a specified rainfall intensity and duration is the first step in characterizing debris-flow risk. Complete characterization of debris-flow risk, in terms of expected losses, would include probabilities that down-channel flow and deposition will encroach upon a particular location (for example, enter a specific cell) and will require additional information about the spatial distributions of people and property values. However, forecasting when and where changes in the probability that debris flows will be initiated during a rainstorm, and the rapid (near real time) map display of the spatial distribution of those probabilities, may be of help to communities in making informed decisions about public warnings and emergency response.

Map approved for publication July 31, 1996.

In December, 1991, at the request of the California State Geologist, the U.S. Geological Survey (USGS) began a study to forecast the risk of rainfall-triggered debris-flow damage in the hills northeast of Oakland, Calif., an area affected by a disastrous fire on October 20, 1991. Although the request was stimulated by the fire disaster, the procedures reported here do not directly address the special effects of fire on hillside materials. Natural hillside vegetation will generally recover within a few years, and eventually achieve a mature condition that can persist for decades. The issue for which we were asked to provide information was not the short-term protection of undamaged property downstream from burned areas, but whether requirements for reconstruction should include mitigation measures to prevent damage from debris flows during the normal expected life of a rebuilt residential structure.[1] This study, therefore, focuses on events that are expected to occur on natural (ungraded) hillsides with mature vegetation.

Mitigation measures, including the grading code provisions of Chapter 70 of the Uniform Building Code (International Conference of Building Officials, 1979), and engineered structures such as those described by Hollingsworth and Kovacs (1981) and Baldwin and others (1987) have been applied by communities in both southern California and the San Francisco Bay region. It was expected that postfire reconstruction offered an opportunity to implement regulations for grading or to require protective structures that might prevent damage from future rainfall-triggered debris flows. The preliminary results of the present probability model, which addresses only the initiation of debris flows, does not include the potential for hazard to a downslope or downstream area from debris flows originating at higher elevation, and may not be sufficient to influence community decisions to regulate for mitigation. However, a capability to map time-dependent changes in the expected abundance of debris flows in different, relatively small drainage basins as rainfall persists, may be applicable to hazard warning and mitigation issues.

It has long been recognized that chaparral fires affect hillside materials in ways that increase the potential for rainfall-triggered debris-flow occurrences immediately following a fire and during a recovery period of a few months to a few years. These effects have been described by researchers such as Wells (1987), Morton (1989), and Spittler (1989). On unburned slopes, there is usually some time delay between the start of storm rainfall and the initiation of the earliest debris flows, and those slopes may respond only to storms having prolonged heavy rainfall. Recently burned areas commonly produce debris flows in response to less intense rainfall and in storms of shorter duration. In storms with prolonged heavy rainfall, which are generally large in area, burned areas commonly yield debris flows earlier than unburned areas. Although the differences in mechanisms are not fully understood, it is possible that further research will permit modification of a probability model to accommodate the changed expectations for the immediate postfire condition.

Previous probabilistic analyses of landslide expectations have been generally static, aimed at developing guides for decisions regarding long-term mitigation (for example, Bernknopf and others, 1988) and possibly used to evaluate the expected benefits of adding mitigation measures to requirements for reconstruction in the disaster area. However, dynamic models of the sort developed in this study, which address temporal and spatial changes in degree of hazard, dependent on the specifics of a given storm, have a potential for short-term applications. A reliable forecast of the times and locations of different degrees of potential hazard might provide a rational basis for short-term evacuation warnings as one form of emergency response. Display of the forecast in map form would aid in clearer communication between emergency response managers and the public.

In this study, we generated a time-dependent statistical hazard function to forecast the probability that a debris flow will be initiated in a specified 100-m × 100-m area (a 100-m cell) after a specified duration of heavy rainfall. The hazard function is an equation that estimates the probability of initiating a rainfall-triggered debris flow at a hillside site after a specified duration of storm rainfall, conditional on no failure having been initiated at that site earlier in the storm. The equation, derived by regression, is used in a GIS environment to calculate estimates of predicted probability of failure in each 100-m cell of a study area in the hills of Oakland, Calif. The GIS environment permits rapid input of map information into computerized analytical procedures and rapid display of analytical results in map form. Indeed, if the spatial data were in place at the beginning of a storm, and storm rainfall were monitored by continuously recording gages, hourly changes in predicted probability could be mapped in near real time.

ACKNOWLEDGMENTS

Special thanks to S.D. Ellen for providing 1982 storm rain gage records from stations near sites where debris flows were observed at known times and to G.F. Wieczorek for many leads to useful data in various articles in USGS Professional Paper 1434. In addition, G.F. Wieczorek, S.D. Ellen, R.K. Mark, and S.H. Cannon provided many helpful discussions about their studies of debris flows triggered by the 1982 storm, and R.K. Mark provided digital map data on post-storm inventories and elevations in the Oakland hills area. Wai-See Moy assisted with early stages of preparation of a preliminary version of the regression data base in LOTUS 123, installed the LIMDEP software, and ran the first regressions in LIMDEP. Susan Price designed ARC/INFO plotting routines that organized the GIS map plots into panels. Jerry Spears, Mathew Falkenstein, and Goeffrey Oppenheimer (the latter two served as USGS volunteers) assisted in preparing data and illustrations. The GIS work was done in the USGS NMD-operated interdivision GIS laboratory in Reston, Va., and we are grateful to L.K. Peng for hardware and software systems administration support. We appreciate reviews by G.F. Wieczorek, D.M. Perkins, and R.W. Jibson of a preliminary abbreviated summary of results (Campbell and Bernknopf, 1993). All aforementioned colleagues are from the USGS. This paper has benefited from reviews by G.F. Wieczorek and R.W. Fleming of the USGS and by A.G. Barrows of the California Division of Mines and Geology. The use of brand names for commercial software is solely to provide an accurate description of procedures, and endorsement by the USGS is neither intended nor implied.

OVERVIEW OF OUR APPROACH

Historically, debris flows originating on natural slopes during prolonged heavy rainfall have posed a substantial threat of per-

[1]Another issue, the short-term protection of undamaged property adjacent to (especially downstream from) burned areas, from debris flows originating in the burned area, was already being vigorously pursued by other Federal agencies, as well as by State and local disaster response agencies, and by private contractors.

Table 1.—Tabular data for the eleven sites of rainfall-triggered debris flows in the San Francisco Bay region that occurred during the storm of January 3–5, 1982. All failures occurred on January 4, 1982, at the time of day shown in 24-hour format

[Time-of-failure (Pacific Standard Time (PST)) is the observed time of the debris flow (generally assumed to be less than 20 minutes after time-of-failure of parent soil slip); duration of survival (hours of rainfall at a rate $I>I_0$) from start of rainfall at rates exceeding threshold rainfall rates, I_0 (which are assigned to the site depending on whether mean annual precipitation is greater than or less than 660 mm (26 in) at the nearest recording rain gage); slope angle at soil-slip scar as reported in case studies or measured from contours; shear resistance estimated from reported observations of soil properties, including geotechnical measurements of strength, where tested; thickness of colluvium as reported in case studies; and an estimate of the number of censored sites in the vicinity of each failed site based on statistical relations reported in Wieczorek and others (1988)]

Site no.	Time-of-failure (PST)	Duration of survival ($I>0.25$ mm/h) (hours)	Duration of survival ($I>I_0$) (hours)	I_0 (mm/h)	Slope	Shear resistance	Thickness of colluvium (m)	Number of censored cells
1	1930	25	18	6.86	30°	30°	4.5	13
2	1310	18	11	6.86	38°	35°	4.3	9
3	2115	28	16	6.86	30°	40°	1.8	13
4	2310	29	14	4.57	26°–39°	40°	3.9	8
5	1900	25	17	6.86	31°	40°	7.7	8
6	2100	28	1	4.57	26°	40°	1.0	9
7	1200	25	6	4.57	20°	40°	2.0	3
8	1400	20	8	6.86	26°	40°	2.0	5
9	1030	23	5	6.86	23°	40°	2.0	4
10	1234	20	10	4.57	26°	40°	.5	11
11	2000	28	17	4.57	17°	30°	1.5	16

sonal injury and property damage in hillside communities in many parts of the world. Researchers have explored a variety of deterministic physical models of the mechanisms by which these flows begin, move to lower elevations, and deposit (for example, Johnson, 1970; Campbell, 1975; Ellen, 1988; Wilson, 1989). A premise that underlies all of the physical models is that prolonged heavy rainfall results in an increased likelihood for debris flows to occur in the area receiving the rainfall. A probability model for the initiation of debris flows during rainstorms can utilize variables of the sort employed by deterministic physical models, even though the probability model itself has no physical counterpart that is more specific than the premise. Statistical analysis was not used to identify the significant explanatory variables because we felt that the deterministic models identified an appropriate set of variables. Although careful geotechnical measurements are not everywhere available, experienced observers tend to include descriptions of properties that are useful for estimating variables known to be of importance in the deterministic models.[2] Statistical analysis was used, primarily, to evaluate the statistical associations of a variety of explanatory variables to specific outcomes in the context of an established probability model.

[2]Of course, some geotechnical variables, such as cohesion, unit weight of soil, and void ratio, were reported from too few individual sites to be used in the regression; nor could they be systematically estimated from descriptions. In addition, the vertical depth of colluvium was used as a surrogate for the depth to a potential failure surface, even though failures occurred on slip surfaces both above and slightly below actual bedrock-colluvium interfaces. The inability to quantify variations in these properties increases the uncertainty with which different levels of susceptibility can be discriminated.

Observations recorded during and after the January 3–5, 1982, storm in the San Francisco Bay region provide a data set, consisting of spatially and temporally significant variables, suitable as duration (or survival) data for hazard function analysis by regression. The 11 sites identified on the index map (fig. 1; figs. 1–8 are on the plate; figs. 9–13 are in this pamphlet) are widely scattered over four San Francisco Bay region counties. The same spatial variables were observed (or could be reasonably inferred from maps and text descriptions) for each site, and the times-of-occurrence of debris flows also were observed and described, chiefly in Ellen and Wieczorek (1988).

Data from eight continuously recording rain gages, each located near (within a few kilometers) one or more of the sites (from S.D. Ellen, written commun., 1992) were used to define the beginnings and ends of periods when the effect of heavy rainfall would be cumulative. These gage records provide measures of the total duration (in hours) of exposure of cells in the vicinity of each gage, as well as the duration of survival (time-to-failure), T, for cells where soil slips occurred. The cumulative rainfall at each gage station, adjusted to show incremental increases only for times that rainfall intensity exceeds threshold minima that depend on the mean annual precipitation at the station (see Cannon and Ellen, 1988), provides a time-varying variable, CRI_T (cumulative rainfall index), that can be calculated from records for rain gages near the sites of failure.

The spatial data from the 11 sites are summarized in table 1, which also shows site numbers for associated continuously recording rain gages and lists the threshold rainfall intensities (I_0) used to calculate the CRI (for detailed information, see Campbell and others, 1994, appendix A, p. 23–27). The length of time from the beginning of heavy rainfall in a storm to the time of

failure, or to the end of the period of observation, provides the duration of survival, *T*, which becomes the dependent variable in a regression on a probability function. Because each incremental increase in the *CRI* that does not result in failure produces a separate observation of the duration of survival, *T*, the resulting data set attains a size that is the product of the number of sites and each time increment[3] between the beginning of the storm and the time of failure at the observed site. The time of failure is also termed the time that a failed cell exits from the set being observed. Unfailed cells in the vicinity of a failed site, that have virtually the same properties and essentially the same exposure as a failed site, are termed censored; they have survived beyond the end of the period of observation (the end of heavy rainfall). Using times-of-failure and times-of-censoring in a probability survival function as the dependent variable, regression yields coefficients for the independent variables and parameters appropriate for calculating the related probability density, distribution, and hazard functions (Kiefer, 1988).

Hillside attributes for the Oakland hills study area were acquired in a GIS from regional maps of geology (fig. 2, on plate), soils (fig. 3, on plate), and a landslide inventory (fig. 4, on plate). Digital line graph (DLG) data for roads, streams, and contours (fig. 5, on plate) were used for the base map. Slope was calculated from the contour DLG (fig. 6, on plate), shear resistance was estimated from the regional geology and landslide inventory data, and thickness of colluvium was approximated from descriptions of soils map units. Records from a nearby rain gage were used to reconstruct the *CRI* curve for the 1982 storm. The hillside attributes and rainfall characteristics were used to calculate the probability estimates in the GIS environment, and the results are displayed in a panel of maps (fig. 7*A–J*, on plate) that show the spatial distribution of probabilities as reconstructed for 4-hour intervals during the storm. A comparison of the distribution of actual failures resulting from that storm (from post-storm inventory mapping reported *in* Ellen and Wieczorek, 1988) with the distribution of probabilities forecast by the model for storm hour 32 (the time of highest hazard function probability in all cells) indicates that the distribution of actual failures constitutes a representative sample of the probability population at that hour (fig. 8, on plate; fig. 9).

Procedures for evaluating the performance of a probability map as a predictor of inventory data differ from the visual comparisons often used for evaluating susceptibility maps that show categories of high, moderate, or low potential for landslide hazard. In a landslide susceptibility map, one expects to find the greatest spatial concentrations of failures in areas designated as having the highest susceptibility, fewer or less concentrated in areas designated as moderate, and very few or none in those of low susceptibility. A map showing a post-storm inventory of debris-flow scars can be compared visually with a susceptibility map by counting the frequency with which inventoried events occur in each susceptibility category. Such a visual comparison may be sufficient to evaluate the performance of the susceptibility map. However, a simple visual comparison may not be appropriate for use with a probability map. The cell-by-cell calculation of probability produces a continuum of unique numbers that must be grouped into discrete intervals for contouring or color map display. (By implication, all the cells in an interval have the mean probability of the cells in that interval, and the difference between cells that fail and those that do not fail is a consequence of random chance.) Each probability interval is a map unit and is expected to have a number of failures that is the product of the mean probability of the interval and the number of cells (area) in the interval. The customary division of a continuum of numbers into equal intervals does not closely approximate customary categories of susceptibility. Therefore, comparing a post-storm inventory of scars with a map that displays a range of probabilities as a small number of discrete probability intervals is not as visually simple as comparing the same inventory with a susceptibility map, *unless* the intervals are selected so that high, moderate, and low categories of susceptibility can also be defined and delineated in probabilistic terms.[4] The intervals used to display the probability maps in this report are a compromise selected to illustrate temporal changes in probability during a storm and to permit some approximate visual comparisons between the peak probabilities (in hour 32 of the storm) with the post-storm inventory of debris-flow scars.

PROBABILITY MODEL

The probability model under study is an adaptation of statistical procedures for the development of hazard functions from the analysis of time-to-failure (or duration of survival) data, summarized by Kiefer (1988). Kiefer attributes the early development of these techniques to industrial engineering, where they have been used to describe the useful lives of various machines, and in the biomedical sciences, to describe events such as the survival times of heart transplant recipients. To paraphrase Kiefer's description, using the probability of a soil-slip–debris-flow event during a spell of heavy rainfall as an example, the central concept is not the unconditional probability of an event taking place (for example, the probability that failure will occur at a specific location after exactly 12 hours of storm rainfall), but the conditional probability of failure in the 12th hour of the storm, given that no failure occurred at that location in the preceding 11 hours.

Hazard function analyses commonly utilize a probability model that can be described by a density function, that is, one having a continuous distribution (Cox and Oakes, 1984, p. 13). Kiefer (1988, p. 649) discusses difficulties in the application of normal and lognormal distributions, describes how a few of the most commonly used parametric probability distributions have been applied to the analysis of duration (or survival) data, and identifies how the behavior of the functions relates to reasonable natural conditions. For example, the constant hazard rate of an exponential distribution (Kiefer, 1988, p. 654) would seem to be inappropriate for rainfall-triggered soil slip-debris flows, because the frequency of debris-flow events is expected to increase with time as high rates of rainfall continue.

[3]Where time is measured in hours, each hour of survival becomes a new observation. Time increments, however, do not need to be equal and, as a practical matter, if a rainfall rate is relatively constant for a period of two or more hours, that multihour period can be used as a single observation.

[4]If, for the probability maps in this study, we define high susceptibility as referring to areas that should include more than 50 percent of the expected failures and low susceptibility as referring to areas that should include fewer than 5 percent of the expected failures, 4 percent probability is equivalent to the lower limit of high susceptibility, 0.5 percent probability is equivalent to the upper limit of low susceptibility, and moderate susceptibility lies between 0.5 and 4 percent probability.

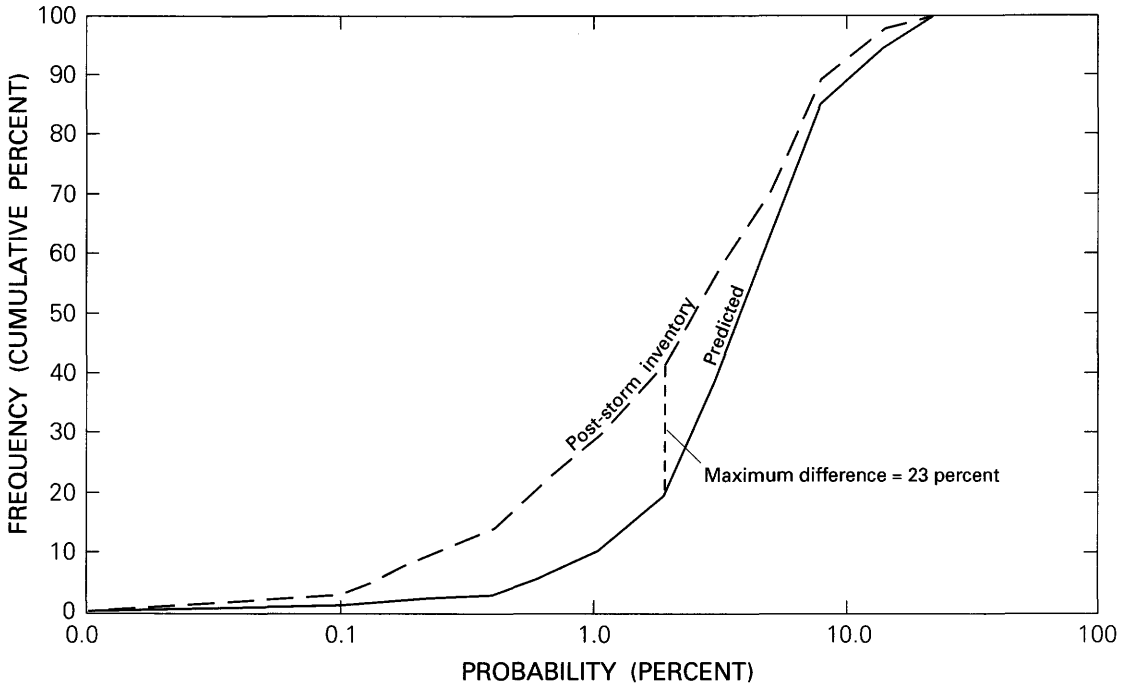

Figure 9.—Cumulative curves comparing frequency of expected failures in the cell population of the map area at hour 32 with post-storm inventory of failures. The Kolmogorov-Smirnov test for goodness-of-fit measures the deviation of the observed cumulative distribution of a sample from the hypothesized cumulative distribution of a population. It tests for type 1 error. If the null hypothesis, H_0, states that the population distribution is the same as the sample distribution, the type 1 error is the probability that H_0 will be rejected when H_0 is correct. For a sample size of 35, a maximum deviation less than 0.23 (23 percent) indicates that rejecting the H_0 will be incorrect with a type 1 error of 0.01.

The test is applied only to cells that have average slopes of 14 degrees or greater because areas that have slopes of less than 14 degrees were excluded from the regression data set by the procedure used to estimate the number of censored cells. Although the hazard function equation can be used to calculate probabilities in all the cells that have data, its application to cells with average slopes of less than 14 degrees is less appropriate than to steeper cells. Rainfall-triggered soil slips were not observed on slopes less than 14 degrees in the 1982 storm (Wieczorek and others, 1988), and soil slips in cells with low average slopes in figure 7 may be attributed to short steep slopes, too short to be captured by the resolution of the digital elevation model.

We specify the conditional probability, P, that a soil slip-debris flow will be initiated during a rainstorm after a given duration, t, at a given place, k, on the condition that no soil slip-debris flow began exactly there earlier in the storm. (In other words, the material that failed at time, T, was in place, unfailed, at time $T-1$.) This condition specifies P as a Markov process[5] that has a discrete state space (s={0,1} slide at k)[6] and a continuous parameter space (time, t={0,1,...,T}) (Bhat, 1984). In this kind of probability model, the rainfall record supplies a clock for time-dependent changes in the probability that a site will survive successive time increments of the storm. As rain persists at a rate exceeding some threshold minimum, the conditional probability that a soil slip-debris flow will occur is expected to rise, and a change in state (from s=0 to s=1) can be viewed as the consequence of time-dependent reductions in stability at k. The model is used to test the null hypothesis,[7] H_0, in equation 1.

$$H_0: P_s^k(T) = P_s^k(0); \text{ where } t=0,1,\ldots,T;\ k=1,\ldots,K \qquad (1)$$

[5]A Markov process is defined as a limited-memory sequence having the property of a one-stage memory. That is, an outcome at the second stage is only dependent on the outcome of the first stage, and not on outcomes at stages prior to the first. For example, if material is removed from a place, k, at time, T, the state of k at $T-1$ must have included the presence of the material, regardless of the states of k at $T-2$, $T-3$, etc.

[6]Soil slip-debris flow either occurs at k (s=1) or does not occur at k

[7]Simply stated, the null hypothesis, H_0, is that the probability of a soil slip-debris flow occurring in any cell, k, at some future time, when $t=T$, during a rainstorm, is the same as the probability at the beginning of the rainstorm, when $t=0$. The alternative hypothesis, H_1, is that the probabilities for the same cell, k, are different for $t=0$ and $t=T$.

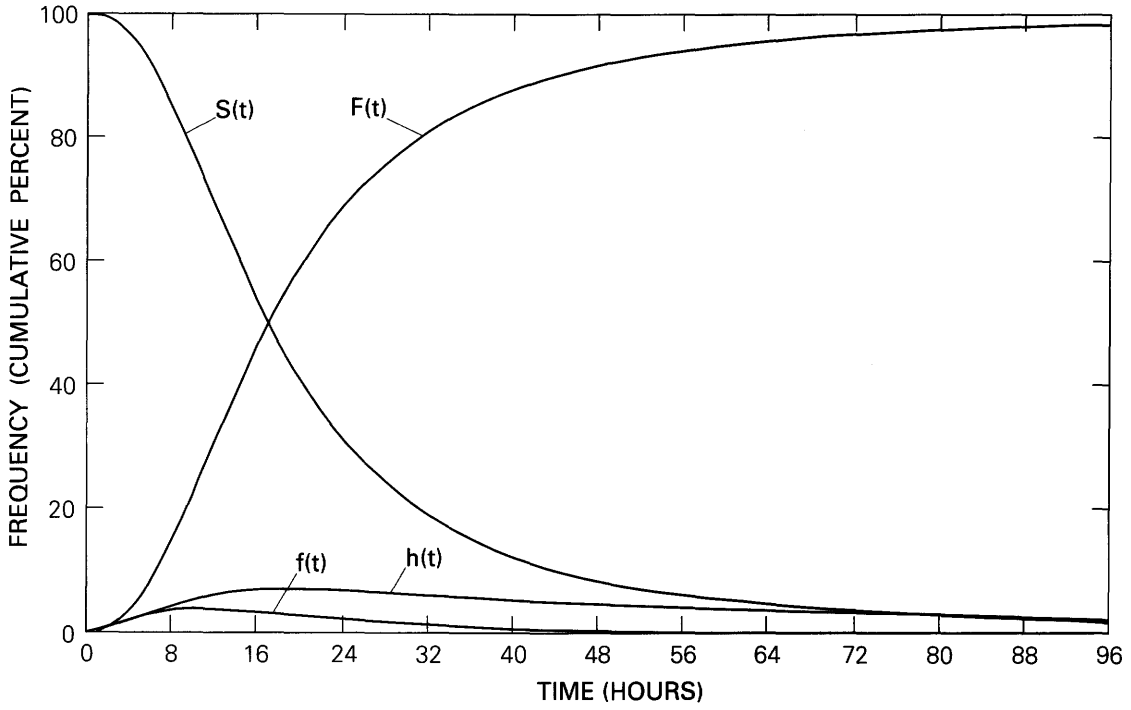

Figure 10.—Logistic functions for the sample (24 hours) extrapolated to 96 hours using mean values for x_i from the regression data set. Survival function, $S(t)=1/(1+(\lambda t)^p)$; probability distribution function, $F(t)=1-S(t)$; probability density function, $f(t)=dF(t)/dt$; and hazard function, $h(t)=f(t)/S(t)=\lambda p(\lambda t)^{p-1}/(1+(\lambda t)^p)$, where λ and p are scale and shape parameters determined by regression.

To prepare an example, we used data available for the exceptional storm of January 3–5, 1982, in the San Francisco Bay region, when times-of-failure were observed for sites of several debris flows (Ellen and Wieczorek, 1988) and applied the model to an area of the Oakland hills.

The conditional probability of initiating a soil slip is derived from a (cumulative) probability distribution of duration, $F(t)=P_s(T\leq t)$, of the current physical state, $s=0$, for which the survivor function is $S(t)=1-F(t)=P_s(T>t)$ (Kiefer, 1988; Lancaster, 1990). The model assumes that the probability of survival continues to decrease with time as high-intensity rainfall continues. Initially, we chose the weibull distribution to model duration data from the 1982 storm because it has the assumed property when the shape parameter, p, is greater than 1 (Campbell and others, 1994). However, subsequent trials and testing led to present use of a logistic distribution, for which the hazard function more closely follows increases and decreases in the *CRI* (Campbell and Bernknopf, 1997). In the notation of Greene (1991, p. 724), the model for the logistic survivor function is equation 2.

$$S(t)=1/(1+(\lambda t)^p);\ \textit{with}\ \lambda=e^{-(\beta_1 x_1+\beta_2 x_2,\ldots,\beta_n x_n)} \qquad (2)$$

where x_i are independent variables (Greene, 1991). The coefficients, ß, and parameter, p, determined in the regression also control the scale and shape, respectively, for the related logistic probability density, probability distribution, and hazard functions (fig. 10).

SPECIFYING THE VARIABLES

The dependent variable is a function of time and requires defining (1) a time of origin, (2) a scale for measuring time, and (3) a failure time that occurs only once for each site (Cox and Oakes, 1984). Cells in which a failure event occurs at an observed time are said to exit from the set of cells that makes up the population under study. The time-dependent functions (fig. 10) assume that sites that survive the period of observation have failure times later than the end of the period of observation, and their durations of survival are termed censored. Clearly, there are several ways to specify the times of origin and ending of a rain storm from rain gage records. In the example reported here, the time of origin of the period of observation is specified as the beginning of a 1-hour (or longer) period in which rainfall intensity exceeds a specified threshold minimum (I_0) at the rain gage nearest to the site of an observed failure. The end of the period of observation is defined by the end of continuous measureable rainfall or a CRI_T of 0, whichever is earlier, at the same gage (see rainfall curves, fig. 11). The duration of survival, therefore, extends to either the time-of-failure (fig. 11), for sites where failure occurred, or beyond the censoring time at the end of storm rainfall (fig. 11), for sites that survived the entire storm. Note that the time of origin for total cumulative storm rainfall may precede the origin time for the period of observation by several hours. As shown on figure 11*B*, the observation period (duration of survival) at gage A–5 begins after 13 hours of recorded continuous rainfall.

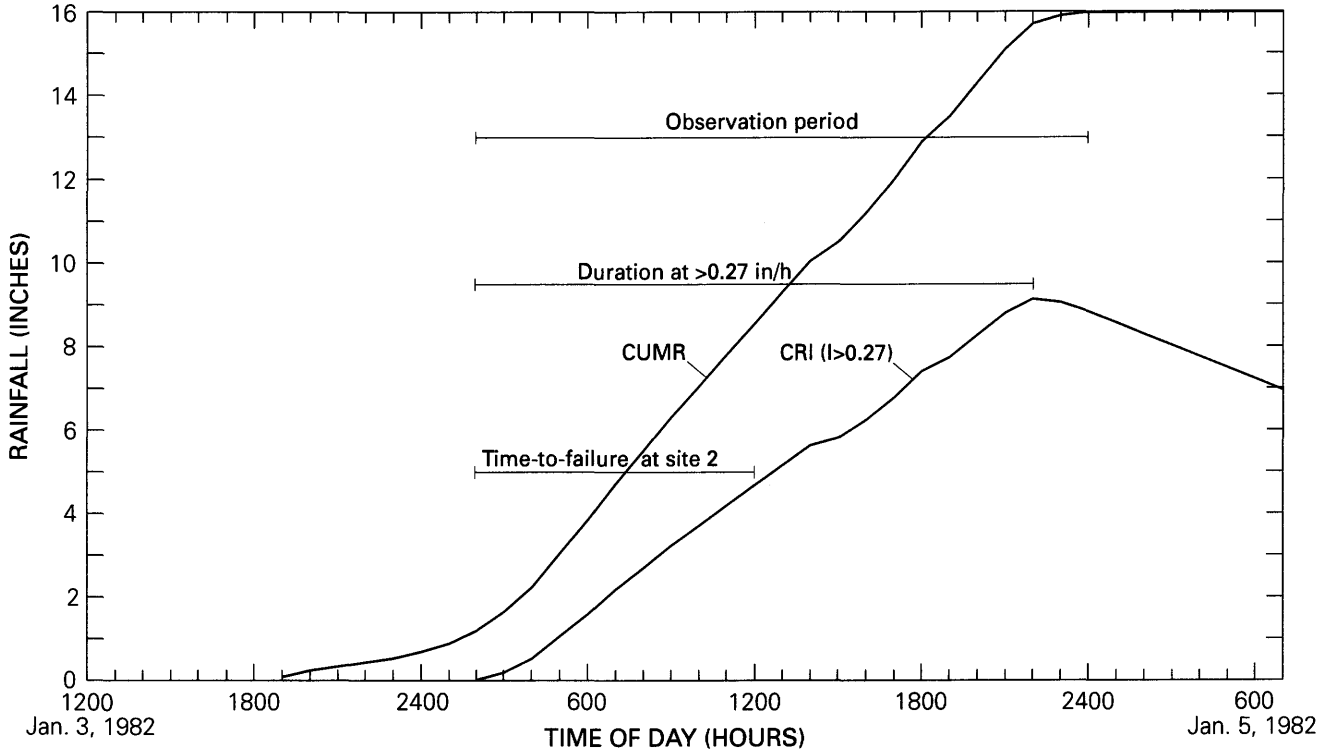

A

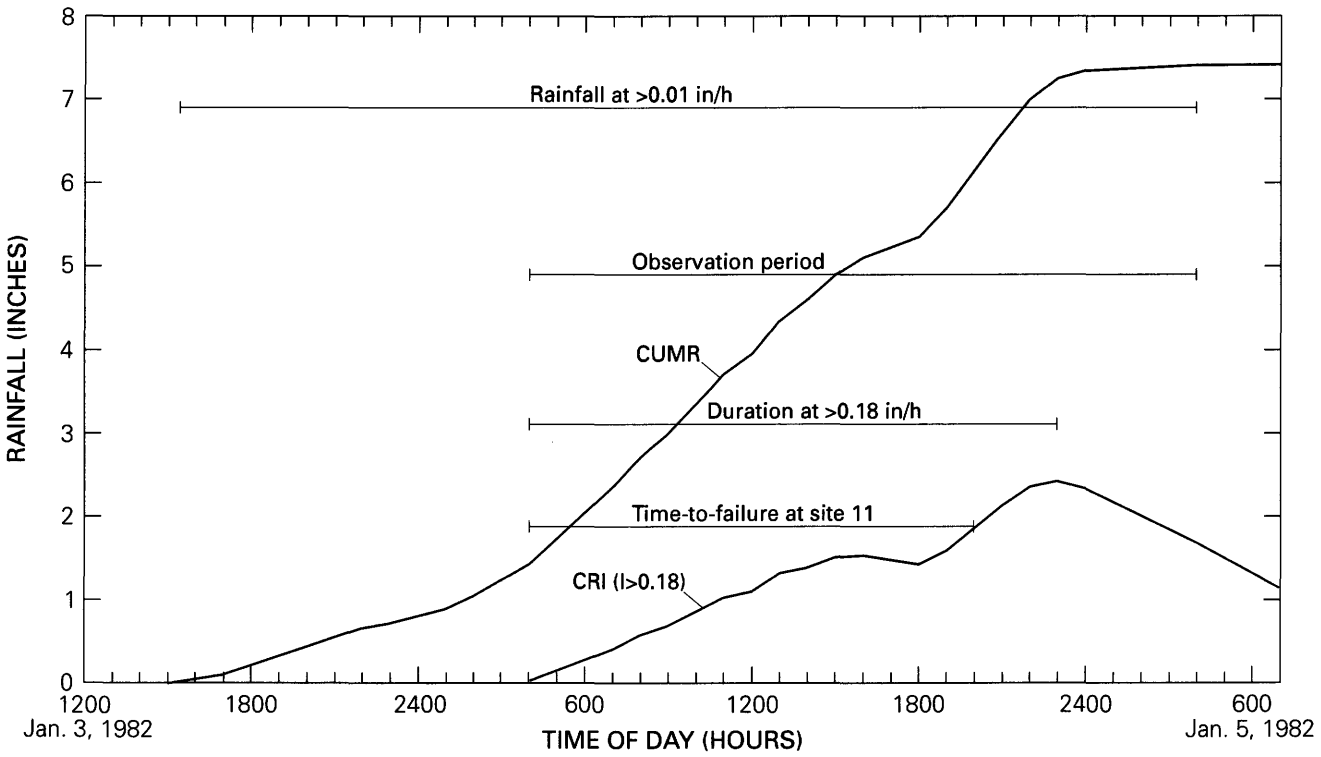

B

Figure 11.—Rainfall curves illustrating the cumulative rainfall index (*CRI*) at two different gages: (***A***) SZ–4, a gage in Santa Cruz County near site 2 in an area that has a high (>660 mm) mean annual precipitation (MAP) and (***B***) A–5, a gage in Alameda County near site 11 in an area that has a low (<660 mm) MAP. At both gages, the upper curve is total cumulative rainfall and the lower curve is cumulative rainfall index from equation 3, using an I_0 of 6.8 mm/h (0.27 in/h) for SZ–4 and an I_0 of 4.6 mm/h (0.18 in/h) for A–5. Time lines show relation of rainfall curves to start and end of observation period, time-to-failure (duration of survival), and duration of continuous rainfall at intensity greater than I_0.

The San Francisco Bay region case studies, which were undertaken for a variety of specific purposes immediately following the storm disaster, did not anticipate the kind of statistical application used in our present study; therefore, none of the San Francisco Bay region case studies reported direct measurements or estimates of the number of censored (survivor) cells in the vicinity of a failed cell. To be included in the same set of cells as a failed cell, a censored cell should have the same spatial attributes (within the range of observation or measurement error) as the cell that failed at a known time. In the absence of direct observations, we estimated a proportion of censored cells in the vicinity of each observed failed cell by extrapolating from statistical data on overall slope frequency and failure frequencies in different slope categories assembled for San Mateo County by Wieczorek and others (1988). Post-storm inventory maps (Ellen and Wieczorek, 1988, pls. 5, 6, and 8–12) provided a partial check on the results. (Details of the procedure are described in Campbell and others, 1994, appendix B, p. 28–29.)

The independent variables of slope, shear resistance, and thickness of colluvium reflect (1) the prestorm stability at each site and (2) the destabilizing effect of rainfall. To use hillside characteristics in a probability model, they must be represented by numbers (for example, slope in degrees or percent). Moreover, the same variables must be reported (or readily inferred from descriptive records) for all the sites contributing to the regression data base and must also be available from the regional map data for areas where the regression equation will be applied. The variables summarized for failure sites in table 1 meet these criteria (for detailed information, see Campbell and others, 1994, appendix A, p. 23–27). However, it seems clear that greater comprehensiveness and more uniform quantitative results would be achieved if additional case study observations were made with the specific objective of measuring and recording the variables used in this statistical analysis.

The independent variables were not identified through statistical factor analyses. They are, instead, analogs of variables that are commonly significant in geotechnical analyses[8] of slope stability, even though calculations based on properties estimated from descriptions and regional map data are clearly *not* geotechnical stability analyses. Slope, shear resistance, and thickness of colluvium are fairly widely reported, or can be inferred from narrative descriptions, for sites where landslides have been studied, and there is a body of scientific and engineering literature modeling their relations to slope stability (see, for example, Morgenstern and Sangrey, 1978). Other workers (for example, Carrara and others, 1978; Mark, 1992) have found some geomorphologic features and vegetation associations to be significant in statistical analyses of factors affecting slope stability. Data on geometric factors, such as planar and profile curvature of landforms, if available, could be incorporated into the regression model. However, including factors such as aspect, vegetation type and density, or various classes of erosional characteristics, would not be consistent with our use of variables analogous to those having recognized applications in geotechnical analysis.

[8]Because the numerical values for the variables are estimates, rather than the results of laboratory or in situ tests, it would be inappropriate to use them in an actual stability analysis. We did not attempt to estimate some variables, such as unit weight and void ratio, for use in the regression data base.

Geotechnical models of slope stability utilize relatively few variables, and these are subject to uncertainty about how accurately they were measured and uncertainty about how well the measurements represent the materials in areas adjacent to a sample locality. If these variables are estimated from site-specific descriptive narratives, uncertainty is significantly increased. And if these variables are estimated from regional map information (without benefit of testing for soil properties at closely spaced sample intervals), uncertainty is even greater. In addition, the areal distribution of rainfall is hardly ever uniform over an area of more than a few square kilometers, and a widely spaced gaging network cannot capture the entire range of rainfall rates or their local distributions. It is not surprising, therefore, that many rainfall-triggered soil slips occur in settings where adjacent, seemingly identical areas remain unfailed at the end of a storm. Presumably, undetected spatial differences in properties or rainfall determine that a failure event will occur in one area and not in another. Where map information is based on reconnaissance, the undetected differences may be large; where the map information is detailed and comprehensive, the undetected differences are expected to be small.

Most site descriptions include either a direct observation of the slope angle or a detailed topographic map from which slope can be calculated for the locations where failures occurred. At a few sites, however, slopes could only be measured from the contours of the 7.5-min quadrangle maps. Within the Oakland hills study area, a digital line graph of the topographic contours was available, providing the basis for a good quality digital elevation model (DEM) at 30-m spacing. From the DEM, slope angles were derived for each 100-m cell in the area (fig. 6, on plate).

An angle of shear resistance was estimated for the colluvium at each of the 11 failure sites. Geotechnical measurements of samples were available only for site 4, where results of direct shear tests are reported as internal friction angles ranging from 26° to 39° (Howard and others, 1988, p. 180). Because test measurements were not generally available, we adopted a systematic procedure to estimate shear resistance from descriptions of the colluvium and underlying parent material. The same procedure could also be applied to regional map data in the Oakland hills. A shear resistance angle of 40° was assigned to colluvium derived from metamorphic rocks, unaltered igneous rocks, or very well indurated sedimentary rocks; 35° was assigned to colluvium derived from moderately indurated sedimentary rocks, including shales; and 30° was assigned to colluvium derived from unconsolidated surficial deposits, including preexisting landslide deposits. These three categories also represent the expectation that the stronger bedrock materials give rise to colluvium that contains larger and more abundant clasts and is, therefore, stronger. The categories fall within the range of angles of shear resistance reported by Terzaghi and Peck (1967, p. 107) for sands and silts. The selection of shear resistance categories was aided by G.F. Wieczorek (written commun., 1992) who, with coauthors (Wieczorek and others, 1985), developed a categorization of shear strengths for analysis of regional slope instability during earthquakes. In the Oakland hills area, categorization of shear resistance was assisted by the observations of Radbruch (1957), Radbruch and Case (1967), and Nilsen (1975), and by descriptions of hillside materials units provided by S.D. Ellen and C.M. Wentworth (written commun., 1992) from a manuscript they were preparing on hillside materials and slopes of the San Francisco Bay region, California (Ellen and Wentworth, 1995). Although our estimation procedure may not be suitable for some

applications, for methods development purposes it does provide consistent preliminary estimates of broad categories of shear resistance in slope materials.

Thickness of colluvium was observed and reported for many of the failure sites summarized in table 1; for the remainder, thickness could be reliably estimated from published photographs and maps, tabulated descriptions of sample locations, or regional associations (see Campbell and others, 1994, appendix A, p. 23–27). Within the Oakland hills study area, thickness was estimated based on the descriptions of soils series map units in reports prepared by the U.S. Soil Conservation Service (Welch, 1977, 1981).

Functional combinations of some variables also were prepared and tested in the regression analysis. An example of a functional combination is the stability index (*SI*) (table 2), defined as the ratio of the tangent of the angle of shear resistance (*SR*) to the tangent of the slope angle (*SLOPE*). This ratio has the form of a dry factor-of-safety, to which it is analogous; but it is clearly not the result of, nor a substitute for, a geotechnical analysis of slope stability.[9]

A separate independent variable represents the cumulative effect of rainfall at time, *T*, as a function of rainfall intensity and duration. Several workers have suggested that debris flows are triggered only after minimum conditions of rainfall intensity and duration have been achieved (for example, Campbell, 1975), and some have suggested functional forms for limiting minimum combinations of intensity and duration (for example, Caine, 1980; Wieczorek and Sarmiento, 1988; Cannon and Ellen, 1988). Keefer and others (1987) have applied empirically derived thresholds to procedures for monitoring a network of telemetered rain gages to provide regional warnings about the potential of an ongoing storm to trigger debris flows in the San Francisco Bay region. The empirical thresholds are thought to represent a dynamic balance between rates of rainfall input to slope-surface materials and output from those materials by deep percolation, lateral drainage, or surface runoff. Where input rates exceed output rates, water can accumulate in the pores and, in sufficient amounts, cause increases in pore pressure and a consequent reduction in shear resistance at a potential slip surface, commonly at or near the base of the colluvium. Wilson (1989) has developed a theoretical deterministic model that describes these physical relations.

Our probability model incorporates the notion of an empirical threshold (or thresholds) in a time-varying variable that is derived from recording rain gage records using a simple difference equation. The equation permits selecting any threshold intensity, I_0, between 0 and the maximum rate recorded at a site. Although we have used constant I_0's in the present study, the difference equation could, if desired, apply a time-dependent function such as that of Caine (1980) or Cannon and Ellen (1988) to determine a threshold intensity for a selected time. The cumulative rainfall index, CRI_T, is a convenient way to characterize a cumulative effect at time, *T*, for bursts of rainfall rates, *I*, in time interval, *t*, that exceed selected minimum rates, I_0 (fig. 11). It is calculated as:

$$CRI_T = CRI_{T-1} + (I_t - I_0)t; \ \textit{Subject to:}\ CRI_T \geq 0 \qquad (3)$$

The I_0's used in preparing the regression data base (see Campbell and others, 1994, appendix D, p. 32–43) are 6.8 mm/h (0.27 in/h) and 4.6 mm/h (0.18 in/h), where gages are in areas having a mean annual precipitation (MAP) greater or less than 660 mm (26 in), respectively (fig. 1, on plate). The use of two thresholds follows the work of Cannon and Ellen (1988) which shows that, in the San Francisco Bay region, areas receiving MAP greater than 660 mm have higher threshold intensities than areas receiving MAP less than 660 mm. In the present study, the specific minima were chosen because, at the observed times of failure, they were exceeded by the rainfall rates at all gages near the failure sites (fig. 11). The CRI_T may be combined with spatially variable hillside characteristics if the independence of the variables is not compromised. For regression and computation in the present example, the CRI_T can be used alone or in combination with the thickness of colluvium (estimated from case studies and soils maps) in a ratio *M* so that the product, *MSI*, is a time-varying fraction of *SI*.

The foregoing variables were selected for specification because they had been observed and reported at case study sites and nearby rain gages, or could be easily estimated from maps and descriptive reports that included the case studies. In addition, the same variables could be estimated from regional data available for selected areas where a probability equation using them might be applied. Although some combined forms, such as the stability index, may be analogous to some simple deterministic geotechnical models, it would be misleading to regard them as physical models. The probability model treats them simply as convenient combinations of individual variables. The probability model would accept more variables (and more complex combinations of variables) if the relevant data were available for both regression and map area application.

REGRESSION

Table 1 lists debris flows that occurred during the storm of January 3–5, 1982, their observed time of occurrence on January 4, thresholds for rainfall rate, I_0, at the nearest recording rain gages, the hillside characteristics at those sites, and an estimate of the number of unfailed (censored) sites in the vicinity of each site of failure. The spatial variables were examined by regression in combination with each of two time-varying variables, cumulative rainfall *CUMR* and *CRI*, both individually and in combination with other spatial variables. Table 2 shows the results of regressions on 20 different sets of variables, including some functional combinations.

Regression on the survival function, equation 2, yields the kinds of coefficients and other statistics tabulated in table 3 for model 20 (table 2). Regressions were run by using the commercial econometrics software package LIMDEP, version 6.0 (Greene, 1991).[10] Regression was repeated for the combinations

[9]The statistical regression is not sensitive to the limit equilibrium implications of the *SI* and recognizes it as simply another set of numbers. Therefore, although the slope and shear resistance variables reported or estimated for site 2 (see table 1; also Campbell and others, 1994, appendix D) yield an *SI* slightly less than 1, the hazard function probabilities for the site are very much less than 100 percent (see Campbell and others, 1994, appendix E).

[10]Campbell and others (1994) provide an example of a LIMDEP regression command, appendix C, p. 30–31; the data file used for regression to a weibull model in the early part of this study, appendix D, p. 32–43; and a LIMDEP report on regression results, appendix E, p. 44–57.

Table 2.—Comparison of different regression models

[Explanatory variables include *CUMR*, cumulative rainfall from start of continuous measurable rainfall; *CRI*, indexed cumulative rainfall (from equation 3); *SLOPE*, tangent of the slope angle at site of initiation; *SR*, tangent of the angle of shear resistance; *CT*, thickness of colluvium; *SI*, stability index, a ratio of *SR* to *SLOPE*; *Mm*, a ratio of *CUMR* to *CT*; *Mi*, a ratio of *CRI* to *CT*. In a t-distribution having 109 degrees of freedom, the critical limit for 90 percent acceptance is 1.28 or higher. All the variables are significant at or above that level in one or more models; however, in six of the models (1, 2, 5, 9, 12, 13) at least one variable is not significant. Four models (1, 2, 7, 8) yield parameters, *p*, less than 1, for which the hazard functions will decrease with time, and are, therefore, incompatible with the underlying premise of increasing probability with increasing duration of intense rainfall. The same four models (1, 2, 7, 8) also show unrealistically short durations of survival (the average at the 11 sites listed in table 1 is 11.2 hours). Of the 12 models remaining, all appear to be statistically acceptable. —, not applicable]

Model	T-ratios for the variables									*p*	Survival distribution (hours)			
	CUMR	*CRI*	*SLOPE*	*SR*	*CT*	*SI*	*Mm*	*Mi*	*MSI*		95%	75%	50%	25%
1. *CUMR*	0.974	—	—	—	—	—	—	—		0.542	0.01	0.35	2.66	20.2
2. *CRI*	—	−0.232	—	—	—	—	—	—	—	.447	.00	.02	.22	2.61
3. *SLOPE, CUMR*	−3.68	—	8.76	—	—	—	—	—	—	1.78	1.45	4.09	7.59	14.1
4. *SLOPE, CRI*	—	−4.28	19.0	—	—	—	—	—	—	2.05	3.16	7.76	13.2	22.6
5. *SR, CUMR*	−.756	—	—	9.31	—	—	—	—	—	2.28	4.78	10.7	17.4	28.2
6. *SR, CRI*	—	2.46	—	32.8	—	—	—	—	—	2.92	7.31	13.8	20.0	29.2
7. *CT, CUMR*	−2.51	—	—	—	4.27	—	—	—	—	.714	.01	.16	.75	3.47
8. *CT, CRI*	—	−3.59	—	—	7.64	—	—	—	—	.815	.01	.12	.44	1.70
9. *SLOPE, SR, CT, CUMR*	−2.69	—	1.60	1.94	.076	—	—	—	—	2.17	3.13	7.32	12.1	20.1
10. *SLOPE, SR, CT, CRI*	—	−2.62	1.84	1.51	4.14	—	—	—	—	2.41	4.56	9.80	15.5	24.4
11. *SLOPE, SR, CUMR*	−1.32	—	1.68	1.92	—	—	—	—	—	2.20	3.51	8.14	13.4	22.1
12. *SLOPE, SR, CRI*	—	−.31	1.71	3.78	—	—	—	—	—	2.76	6.36	12.4	18.5	27.5
13. *SI, CUMR*	1.25	—	—	—	—	11.1	—	—	—	2.38	6.22	13.5	21.5	34.1
14. *SI, CRI*	—	12.9	—	—	—	45.2	—	—	—	3.68	10.6	17.5	23.6	31.8
15. *SI, CT, CUMR*	−3.39	—	—	—	5.93	12.8	—	—	—	2.22	3.02	6.93	11.4	18.6
16. *SI, CT, CRI*	—	1.53	—	—	5.21	33.7	—	—	—	3.16	8.26	14.8	21.0	29.7
17. *SI, Mm*	—	—	—	—	—	36.2	−3.96	—	—	2.38	4.94	10.7	17.0	26.9
18. *SI, Mi*	—	—	—	—	—	38.6	—	−4.23	—	2.28	4.64	10.4	16.9	27.3
19. *SI, MSI=Mm × SI*	—	—	—	—	—	36.0	—	—	−4.11	2.44	5.14	10.9	17.2	26.9
20. *SI, MSI=Mi × SI*	—	—	—	—	—	39.3	—	—	−4.27	2.32	4.82	10.7	17.2	27.6

Table 3.—Regression results for model 20 (*SI, MSI*), where $MSI=(CRI_T/(39 \times CT)) \times SI$

[Both variables are significant, and the coefficients have the expected signs. These coefficients and parameter, *p*, are those used in equation 4 to calculate the conditional (hazard function) probabilities shown in fig. 7*A–J* (on plate). Log-likelihood = −407.4; $p = 2.32$; $\lambda = 0.06$; median time to failure = 17 hours; correlation coefficient for *SI, MSI* = 0.04]

Variable	Coefficient (β)	T-ratio	Mean	Standard deviation
SI	1.95	39.3	1.48	0.34
MSI	−2.11	−4.27	.117	.20

of variables listed in table 2. Six of the models (1, 2, 5, 9, 12, 13) include one or more variables for which t-ratios are below the critical limit (1.28) for 90 percent acceptance. Four models (1, 2, 7, 8) yield shape parameters, *p*, that are less than 1.0 and produce inappropriate percentile distributions for survival; these models, therefore, yield probabilities that decrease with duration of high-intensity rainfall from an instantaneous high at hour 1, which is not compatible with the premise that higher frequencies of debris-flow events are expected to occur with greater duration of high-intensity rainfall. The curve for model 14 (*SI, CRI*) has $p = 3.68$, which provides for a slow increase in failure probability during the early hours of the storm, but the probability of survival drops to zero after only about 64 hours, the shortest survival time among the four models. The curve using *SI* and *MSI* (where $M=CRI_T/39 \times CT$) shows the shape and scale that seems to best reproduce the observed data. For this model, the variables are conveniently expressed in the same physical units, their correlation coefficient is low, and their signs relate them in a manner analogous to a physical model in which initial stability, *SI*, is incrementally reduced by a fraction, *MSI*, that is a function of rainfall rate and duration. Therefore, we selected this model for use in calculating the time-dependent spatial distribution of probabilities in the area chosen for mapping.

MAPPING SOIL-SLIP–DEBRIS-FLOW PROBABILITY

The coefficients and parameters determined by the regression are then used to calculate hazard function probability estimates for each cell *(k)* in the Oakland hills study area for each hour of the storm. For the selected model, the hazard function, *h(t)*, is

$$h=\lambda p(\lambda t)^{p-1}/(1+(\lambda t)^p); \text{ where } p = 2.32, \lambda = e^{-(1.95SI-2.11MSI)} \quad (4)$$

Map data, as plotted in figs. 2–5 (on plate) were prepared digitally as covers in ARC/INFO, version 5.1, for the northwestern quarter of the Oakland East 7.5-min quadrangle. Rain gage data from gage station A–5 were used to reconstruct the *CRI* and *CUMR* curves (fig. 11*B*) for the January 3–5, 1982, storm as representative of the study area. Base map data are from USGS digital line graphs (DLG's) for roads, streams, and contours in the quadrangle. The contour DLG was used to prepare a digital elevation model from which a shaded relief map (fig. 5, on plate) and a slope map (fig. 6, on plate) were derived. Geologic map units (fig. 2, on plate) were digitized from the map of Radbruch (1969), and additional landslides and surficial features, such as quarry areas (fig. 4, on plate), were digitized from the landslid inventory of Nilsen (1975). Angles of shear resistance were the assigned to each of the map units, following the procedur described in the section on Specifying the Variables and calcu lated into the polygon attribute tables (.PAT's) of the map covers Soils map units for Alameda and Contra Costa Counties (Welch 1977, 1981) were digitized, joined, and reprojected (fig. 3 or plate). From the descriptions of the soils units, average thick nesses were assigned to the map units and calculated into the .PAT of the map cover.

All maps were prepared (reprojected where necessary) in the same projection (Universe Transverse Mercator). Initially, in version 5.1 of ARC/INFO, a cover consisting of an empty mesh of 100-m cells was generated for the area and successively intersected with the slope, geologic, landslide, and soils maps. Slope, shear resistance, and thickness of colluvium were then calculated from the intersected covers into the related .PAT of the empty mesh of cells. Where intersected cells contained two or more subdivisions, each containing different values, an area-weighted average was calculated and transferred to the appropriate mesh cell. Calculations of probability for each selected hour of the 1982 storm were carried out in INFO and placed into the .PAT of the mesh cover. (Campbell and others, 1994, appendix F, p. 58–61, lists the macro command files used to compute the probabilities in INFO.) For subsequent revisions, more recent versions of ARC/INFO including the GRID subroutine were available; the map data were converted to grids of 100-m cells and the calculation of probabilities was done by using grid functions. The spatial distributions of the predicted conditional probabilities for 10 selected hours are shown in the panel of maps reconstructing the effects of the 1982 storm (fig. 7*A–J*, on plate).

DISCUSSION

The resulting maps show the distribution and abundance of cells having conditional probabilities that fall within specified probability categories. The categories represent a range of probabilities, and a mean and a variance can be established for each category. The probability that a debris flow will be initiated in a specific cell, as calculated from equation 4, is not a quantity that can be directly measured by field observation in the cell itself. Although the probability model incorporates relations that are analogous to the way some geotechnical models of natural forces can become unbalanced and trigger landslides, the cell-by-cell probabilities are obviously not equivalent to geotechnical analyses

of site stability. They do, however, provide a way to composite map information into a quantitative expression of the spatial distribution of the likelihood of a debris flow being initiated in sets of equal-area cells. Knowing the probability for a single cell at a specific time has little significance without reference to other cells in the spatial population and to other times. Knowing that a cell has a failure probability of 0.010 (1.0 percent), indicates that of 100 cells having the same probability, one will be expected to fail; but not which one of the 100 it will be. Similarly, a group of 1,000 cells having a probability of 0.001 (0.1 percent) can be expected to have the same number of failures (one). Therefore, the expectation of failure is a function of area as well as of probability. Of course, it is unlikely that equation 4 will yield identical probabilities for any sizeable number of cells.[11] However, uncertainties arising from incomplete knowledge of the spatial and time-varying variables, in part quantified by the variances assigned to the coefficients for the variables, suggest that cells can be grouped into a restricted number of probability ranges, each of which can be represented by a mean probability. Campbell and Bernknopf (1997) have addressed several aspects of the selection of ranges that yield map units of possible interest for different objectives.

In reading and interpreting gridded probability maps, it may be useful to bear in mind that the definition of the probability of an event can be stated (Weaver, 1963, p. 74) as follows: "The probability of an event E is defined by the equation:

$$P(E) = \frac{n}{N} \tag{5}$$

where N is the total number of equally probable outcomes, and n is the number of outcomes which constitute the event E." Therefore, in a population of hillside cells, there is a subset, $N_{T,i}$, having probabilities at time T within a probability interval for which the number of expected failures is $n_{T,i}$. Note that all categories having means that are neither 1.0 nor 0.000000 are expected to have a number of failed cells at time T that is the number of cells in the category ($N_{T,k}$) multiplied by the mean probability of cells in the interval, that is:

$$n_{T,k} = N_{T,k} \times P_{T,k}(E) \tag{6}$$

This provides a basis for comparing the probabilities estimated by equation 4 to observed events, permitting statistical measures of the predictive capabilities. By counting the number of inventoried failures (cells with one or more failure) in each probability group, and comparing the cumulative distribution of inventoried failures with the cumulative distribution of expected failures, statistical tests for goodness-of-fit can be applied. Campbell and Bernknopf (1997) used these procedures to compare results using different threshold rainfall intensities to define a time of origin for the period of observation and using different probability distributions for regression. Their results led to two important modifications to the model initially explored by Campbell and others (1994): (1) The time of origin for the period of observation has been redefined to begin when rainfall exceeds the threshold rates selected for equation 3 and (2) a logistic distribution has replaced the weibull distribution. The redefined time of origin for the observation period combined with the change to a logistic distribution yields a better fit to the observed data on time-of-failure than the weibull distribution (fig. 12), without causing a significant reduction in the fit to the spatial distribution of inventoried failures in the study area (fig. 13).

A Kolmogorov-Smirnov test[12] can be applied to the graphs (figs. 12 and 13) to quantify comparisons of the distribution of expected failures for the storm hour in which probabilities are highest with the distribution of failures as inventoried after the end of the 1982 storm. Figure 12 compares hourly changes in frequency of expected failures (calculated for various models, using the means of the variables in the regression data) with the hourly changes in frequency of debris-flow events reported by Cannon and Ellen (1988).[13] The maximum difference in frequency (probability) between the expected failures (according to the model being tested) and the inventoried failures is the Kolmogorov-Smirnov test statistic for 25 degrees of freedom. Figure 13 compares, for the Oakland hills study area, the cumulative relative spatial frequency distribution of cells expected to have one or more failures in hour 32 of the storm (hour 21 of the duration of survival), which is the hour in which hazard function probability is highest, with the cumulative relative frequency distribution of failures identified in a post-storm inventory. Again, the maximum difference in frequency (expressed as probability) is the Kolmogorov-Smirnov test statistic. Figure 13 shows that the frequency distribution of predicted probabilities in cells having one or more inventoried soil-slip scars is similar to the frequency distribution of predicted probabilities in the entire cell population for hour 32 of the storm.

The six probability intervals used for simple colored map units, <0.5 percent, 0.5–1.7 percent, 1.7–4.8 percent, 4.8–7.0 percent, 7.0–8.8 percent, and >8.8 percent, (fig. 7*A–J*, on plate) approximate the <0.5, 0.5–5.0, 5.0–25, 25–50, 50–75, and >75 percent intervals for expected failed cells, which might be considered equivalent to very low, low, moderate, high, and very high susceptibility. Map units of this kind permit some visual comparison with the post-storm inventory (see Campbell and Bernknopf, 1997). This scale of probability intervals is used for map display to permit some visual comparison with susceptibility maps made by other procedures. It also illustrates how probabilistic procedures can quantify and subdivide broad categories of landslide susceptibility.

---

[11]The range of model probabilities, 0.0000–0.1077, can be divided into as many as 200 equal-interval groups, each of which includes at least one cell. The largest of these groups contains 91 cells, is in the probability range 0.0000–0.0006, and has a mean probability of 0.0003 and a standard deviation of 0.0002.

[12]The Kolmogorov-Smirnov test for goodness-of-fit, shown in figure 12, measures the deviation of an observed cumulative distribution of a sample (the post-storm inventory) from the hypothesized cumulative distribution of a population (the predicted probabilities for hour 32). It tests for type 1 error; in other words, if the null hypothesis, H_0, states that the population distribution is the same as the sample distribution, the type 1 error is the probability that H_0 will be rejected when H_0 is correct. For a sample size of 36 cells having one or more inventoried scars, a maximum deviation of 0.23 indicates that the probability of being correct in rejecting H_0 is less than 0.01.

For general discussions of applications of the Kolmogorov-Smirnov test, see standard texts such as Lindgren and McElrath (1967, p. 151–153), Davis (1986, p. 99–101), or Soong (1981, p. 322–325).

[13]Eight of the 11 sites used to provide data for the regression are included in the set of 26 observed debris flows reported by Cannon & Ellen (1988, p. 29).

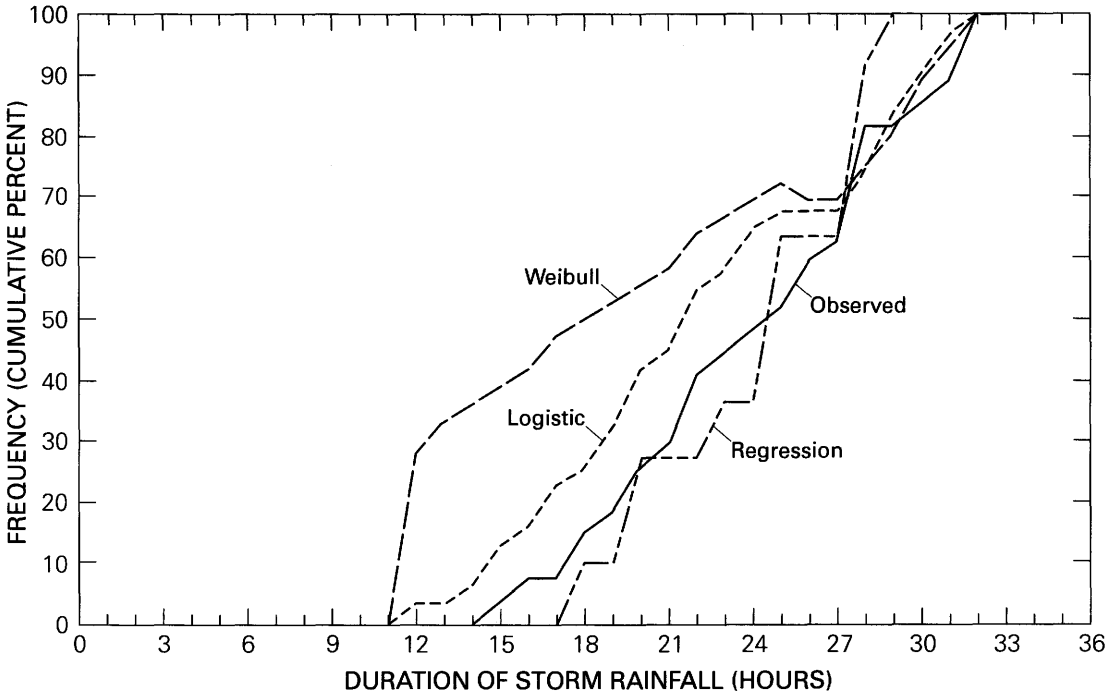

Figure 12.—Hourly changes in expected failures in the northwestern quarter of the Oakland East quadrangle compared with the time-to-failure observations reported by Cannon and Ellen (1988) for 26 sites scattered over all the counties of the San Francisco Bay region. "Weibull" and "logistic" show changes in cumulative frequency of expected failures from the two probability models; "observed" shows cumulative frequency of 26 observed times of failure from Cannon and Ellen (1988); and "regression" shows the cumulative frequency of times of failure at the eleven sites used in the regressions, most of which are included in "observed."

The procedure we have developed yields the conditional probability that a soil slip will occur in a map cell at a time T during a storm if (1) no failure has occurred in that cell before T and (2) rainfall continues at a rate in excess of a selected threshold until T. The Kolmogorov-Smirnov test indicates that the null hypothesis of equation 1 should be rejected. Although the predicted probabilities are clearly not equivalent to deterministic predictions that specific sites will fail or will not fail, and the accuracy of this preliminary model leaves room for much improvement, the Kolmogorov-Smirnov test indicates that the probabilities estimated by a simple time-dependent model produce a curve for frequency of expected failures that is a reasonable match for the frequency distribution curve for observed failures. The procedure also provides a rigorously defined framework for comparing the results achieved by adding new variables or combinations of explanatory variables (as, for example, in table 2) or for comparing the results yielded by applying the same equation in different regions.

Because the equation for estimating time-dependent probabilities as displayed on the maps (fig. *7A–J*, on plate) was built by regression on rainfall and landslide data for the 1982 storm in the San Francisco Bay region, it may be less valid as a forecast tool for soil-slip–debris-flow events where applied to other storms and other regions, which should be tested individually. However, because the rainfall at each case study site is characterized from a separate gage record (except for three instances where two sites are associated with one gage), the function is theoretically independent of a particular storm or region, and statistical bias could be reduced by adding to the regression data base information from case studies from other regions and other storms. The accuracy of the results could probably be improved by adding some specific observations to those commonly recorded in case studies (for example, direct observation of the proportion of unfailed slope areas in the vicinity of a studied failure site).

The results reported here are preliminary, and could be improved by further study. From figure 11, it is clear that both the weibull and logistic models reproduce the frequency distribution of inventoried failures much better in the higher probability intervals (representing high susceptibility) than in the lower half of the probability range (moderate and low susceptibility). Perhaps some other probability distribution (for example, a gamma function) would perform incrementally better than the logistic distribution. Additional spatial variables (for example, permeability, void ratio, and so on) might be acquired and included to develop a more complex model or set of models. More case studies (including representatives of other regions and other storms) could be added to the regression data base, and more accurate ways to estimate regional variations in slope, shear resistance, and colluvium thickness may be devised. The shape and scale of the functions are sensitive to (1) variations in the proportion of censored (unfailed) to exited (failed) cells having the same attributes, (2) the

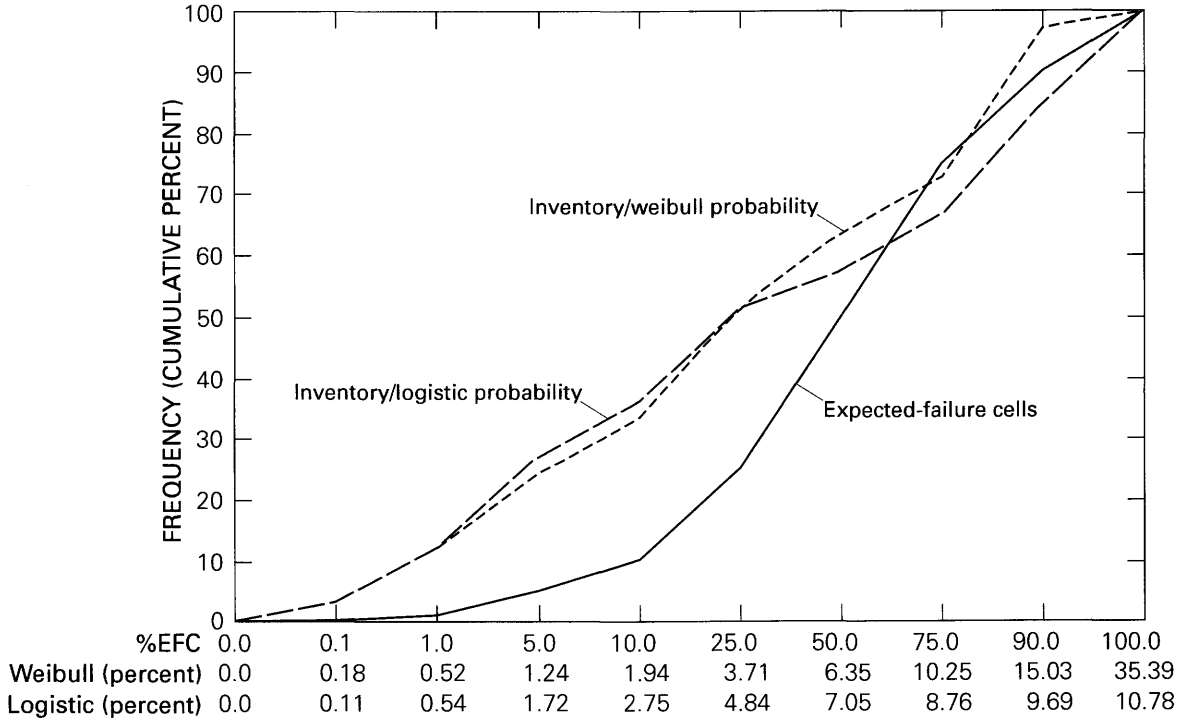

Figure 13.—Graph comparing distributions of inventoried failures in logistic and weibull probability intervals with distribution of expected-failure cells (from equation 4 and interval area) for storm hour 32 (*CRI* hour 21) of the January 3–5, 1982, storm in the northwestern quarter of the Oakland East quadrangle. The x-axis is scaled to a nonlinear distribution of expected-failure cells (%EFC) and shows the maximum weibull and logistic model probabilities that mark the limits of equivalent expected-failure frequency intervals.

specification of the observation period, (3) the geomorphic and geologic properties selected for regression, and (4) the I_0 selected for calculation of the CRI_T. Clearly, better observational input should improve the model. However, the present results encourage further exploration of this and similar models, and their potential, if linked with spatial and temporal socioeconomic variables, to identify and delineate rainfall-induced short-term increases in debris-flow risk.

REFERENCES CITED

Baldwin, J.E., II, Donley, H.F., and Howard, T.R., 1987, On debris flow/avalanche mitigation and control, San Francisco Bay area, California: Reviews in Engineering Geology, v. 7, p. 223–236.

Bernknopf, R.L., Campbell, R.H., Brookshire, D.S., and Shapiro, C.D., 1988, A probabilistic approach to landslide hazard mapping in Cincinnati, Ohio, with applications for economic evaluation: Bulletin of the Association of Engineering Geologists, v. 25, no. 1, p. 39–56.

Bernknopf, R.L., Brookshire, D.S., Soller, D.R., McKee, M.J., Sutter, J.F., Matti, J.C., and Campbell, R.H., 1993, Societal value of geologic maps: U.S. Geological Survey Circular 1111, 53 p.

Bhat, U.N., 1984, Elements of applied stochastic processes (2d ed.): New York, John Wiley and Sons, Inc., 685 p.

Caine, Nel, 1980, The rainfall intensity-duration control of shallow landslides and debris flows: Geografiska Annaler, v. 62A, no. 1–2, p. 23–27.

Campbell, R.H., 1975, Soil slips, debris flows, and rainstorms in the Santa Monica Mountains and vicinity, southern California: U.S. Geological Survey Professional Paper 851, 51 p.

Campbell, R.H., and Bernknopf, R.L., 1993, Time-dependent landslide probability mapping, *in* Shen, Hsieh Wen, Su, S.T., and Wen, Feng, eds., 1993 National Conference on Hydraulic Engineering, Hydraulic Engineering; Proceedings of the National Conference on Hydraulic Engineering, San Francisco, California, July 25–30, 1993, p. 1902–1907.

———1997, Debris-flow hazard map units from gridded probabilities, *in* Chen, Cheng-lung, ed., Debris-flow hazards mitigation; Mechanics, prediction, and assessment, Proceedings of First International Conference..., San Francisco, California, August 7–9, 1997: New York, American Society of Civil Engineers, p. 165–175.

Campbell, R.H., Bernknopf, R.L., and Soller, D.R., 1994, Mapping time-dependent changes in soil slip-debris flow probability: U.S. Geological Survey Open-File Report 94–699, 66 p., 2 pls., scale 1:24,000 and 1:40,000.

Cannon, S.H., 1988, Regional rainfall-threshold conditions for abundant debris-flow activity, chap. 4 *of* Ellen, S.D., and Wieczorek, G.F., eds., Landslides, floods, and marine effects of the storm of January 3–5, 1982, in the San Francisco

Bay region, California: U.S. Geological Survey Professional Paper 1434, p. 35–42.

Cannon, S.H., and Ellen, S.D., 1988, Rainfall that resulted in abundant debris-flow activity during the storm, chap. 3 *of* Ellen, S.D., and Wieczorek, G.F., eds., Landslides, floods, and marine effects of the storm of January 3–5, 1982, in the San Francisco Bay region, California: U.S. Geological Survey Professional Paper 1434, p. 27–33.

Carrara, A., Catalano, E., Sorriso-Valvo, M., Reali, C., and Osso, I., 1978, Digital terrain analysis for land evaluation: Geologia Applicata e Idrogeologia, v. 13, p. 69–127.

Cox, D.R., and Oakes, D., 1984, Analysis of survival data: London, Chapman and Hall, 201 p.

Davis, J.C., 1986, Statistics and data analysis in geology (2d ed.): New York, John Wiley and Sons, Inc., 646 p.

Ellen, S.D., 1988, Description and mechanics of soil slip/debris flows in the storm, chap. 6 *of* Ellen, S.D., and Wieczorek, G.F., eds., Landslides, floods, and marine effects of the storm of January 3–5, 1982, in the San Francisco Bay region, California: U.S. Geological Survey Professional Paper 1434, p. 63–112.

Ellen, S.D., and Wentworth, C.M., 1995, Hillside materials and slopes of the San Francisco Bay region, California: U.S. Geological Survey Professional Paper 1357, 215 p., 7 pls., scale 1:125,000.

Ellen, S.D., and Wieczorek, G.F., eds., 1988, Landslides, floods, and marine effects of the storm of January 3–5, 1982, in the San Francisco Bay region, California: U.S. Geological Survey Professional Paper 1434, 310 p.

Ellen, S.D., Cannon, S.H., and Reneau, S.L., 1988, Distribution of debris flows in Marin County, chap. 7 *of* Ellen, S.D., and Wieczorek, G.F., eds., Landslides, floods, and marine effects of the storm of January 3–5, 1982, in the San Francisco Bay region, California: U.S. Geological Survey Professional Paper 1434, p. 113–131.

Greene, W.H., 1991, LIMDEP user's manual and reference guide, version 6.0: Bellport, N.Y., Econometrics Software, Inc., 893 p.

Hollingsworth, Robert, and Kovacs, G.S., 1981, Soil slips and debris flows; Prediction and protection: Association of Engineering Geologists Bulletin, v. 18, no. 1, p. 117–128.

Howard, T.R., Baldwin, J.E., II, and Donley, H.F., 1988, Landslides in Pacifica, California, caused by the storm, chap. 9 *of* Ellen, S.D., and Wieczorek, G.F., eds., Landslides, floods, and marine effects of the storm of January 3–5, 1982, in the San Francisco Bay region, California: U.S. Geological Survey Professional Paper 1434, p. 163–183.

International Conference of Building Officials, 1979, Uniform Building Code: Whittier, Calif., 780 p.

Johnson, A.M., 1970, Physical processes in geology: San Francisco, Freeman, Cooper and Company, 577 p.

Keefer, D.K., Wilson, R.C., Mark, R.K., Brabb, E.E., Brown, W.M., III, Ellen, S.D., Harp, E.L., Wieczorek, G.F., Alger, C.S., and Zatkin, R.S., 1987, Real-time landslide warning during heavy rainfall: Science, v. 238, p. 921–925.

Kiefer, N.M., 1988, Economic duration data and hazard functions: Journal of Economic Literature, v. 26, p. 646–679.

Lancaster, T., 1990, The econometrics analysis of transition data: New York, Cambridge University Press, 352 p.

Lindgren, B.W., and McElrath, G.W., 1967, Introduction to probability and statistics: New York, The MacMillan Company, 288 p.

Mark, R.K., 1992, Map of debris-flow probability, San Mateo County, California: U.S. Geological Survey Miscellaneous Investigations Series Map I–1257–M, scale 1:62,500.

Mark, R.K., and Newman, E.B., 1988, Rainfall totals before and during the storm; Distribution and correlation with damaging landslides, chap. 2 *of* Ellen, S.D., and Wieczorek, G.F., eds., Landslides, floods, and marine effects of the storm of January 3–5, 1982, in the San Francisco Bay region, California: U.S. Geological Survey Professional Paper 1434, p. 17–26.

Morgenstern, N.R., and Sangrey, D.A., 1978, Methods of stability analysis, *in* Schuster, R.L., and Krizek, R.J., eds., Landslides, analysis and control: Special Report 176, Transportation Research Board, National Research Council, Washington, D.C., p. 155–171.

Morton, D.M., 1989, Distribution and frequency of storm generated soil slips on burned and unburned slopes, San Timoteo badlands, southern California, *in* Sadler, P.M., and Morton, D.M., eds., Landslides in a semi-arid environment: Publications of the Inland Geological Society, v. 2, p. 279–284.

Nilsen, T.H., 1975, Preliminary photointerpretation map of landslide and other surficial deposits of the Oakland East 7.5 minute quadrangle, Contra Costa and Alameda Counties, California, sheet 41 *of* Preliminary photointerpretation maps of landslide and other surficial deposits of 56 7½-minute quadrangles in the southeastern San Francisco Bay region, Alameda, Contra Costa, and Santa Clara counties, Calif.: U.S. Geological Survey Open-File Report 75–277, scale 1:24,000.

Radbruch, D.H., 1957, Areal and engineering geology of the Oakland West quadrangle, California: U.S. Geological Survey Miscellaneous Geologic Investigations Map I–239, scale 1:24,000.

———1969, Areal and engineering geology of the Oakland East quadrangle, California: U.S. Geological Survey Geologic Quadrangle Map GQ–769, scale 1:24,000.

Radbruch, D.H., and Case, J.E., 1967, Preliminary geologic map and engineering geologic information, Oakland and vicinity, California: U.S. Geological Survey Open-File Report, 2 sheets, scale 1:24,000.

Rantz, S.E., 1971, Mean annual precipitation and precipitation depth-duration-frequency data for the San Francisco Bay region, California: U.S. Geological Survey San Francisco Bay Region Environment and Resources Planning Study, Basic Data Contribution 32, 23 p., scale 1:500,000.

Slosson, J.E., and Krohn, J.P., 1982, Southern California landslides of 1978 and 1980, *in* Storms, floods, and debris flows in southern California and Arizona, 1978 and 1980, Proceedings of a symposium, September 17–18, 1980: Washington, D.C., National Academy Press, p. 291–304.

Soong, T.T., 1981, Probabilistic modeling and analysis in science and engineering: New York, John Wiley and Sons, Inc., 384 p.

Spittler, T.E., 1989, Geologic hazard evaluation of the vegetation management plan proposed for Mount Tamalpais, Marin County, California, *in* Sadler, P.M., and Morton, D.M., eds., Landslides in a semi-arid environment: Publications of the Inland Geological Society, v. 2, p. 265–278.

Terzaghi, Karl, and Peck, R.B., 1967, Soil mechanics in engineering practice: New York, John Wiley and Sons, Inc., 729 p.

Weaver, Warren, 1963, Lady luck; The theory of probability: Garden City, N.Y., Doubleday & Company, Inc., 392 p.

Welch, L.E., 1977, Soil survey of Contra Costa County, California: U.S. Soil Conservation Service, 122 p., 54 map sheets, scale 1:24,000.

———1981, Soil survey of Alameda County, California, western part: U.S. Soil Conservation Service, 103 p., 8 map sheets, scale 1:24,000.

Wells, W.G., II, 1987, The effects of fire on the generation of debris flows in southern California: Reviews in Engineering Geology, v. 7, p. 105–114.

Wentworth, C.M., Ellen, Stephen, Frizzell, V.A., Jr., and Schlocker, Julius, 1985, Map of hillside materials and description of their engineering character, San Mateo County, California: U.S. Geological Survey Miscellaneous Investigations Series Map I–1257–D, scale 1:62,500.

Wieczorek, G.F., and Sarmiento, John, 1988, Rainfall, piezometric levels, and debris flows near La Honda, California, in storms between 1975 and 1983, chap. 5 *of* Ellen, S.D., and Wieczorek, G.F., eds., Landslides, floods, and marine effects of the storm of January 3–5, 1982, in the San Francisco Bay region, California: U.S. Geological Survey Professional Paper 1434, p. 43–62.

Wieczorek, G.F., Wilson, R.C., and Harp, E.L., 1985, Map showing slope stability during earthquakes in San Mateo County, California: U.S. Geological Survey Miscellaneous Investigations Series Map I–1257–E, scale 1:62,500.

Wieczorek, G.F., Harp, E.L., Mark, R.K., and Bhattacharyya, A.K., 1988, Debris flows and other landslides in San Mateo, Santa Cruz, Contra Costa, Alameda, Napa, Solano, Sonoma, Lake, and Yolo Counties, and factors influencing debris-flow distribution, chap. 8 *of* Ellen, S.D., and Wieczorek, G.F., eds., Landslides, floods, and marine effects of the storm of January 3–5, 1982, in the San Francisco Bay region, California: U.S. Geological Survey Professional Paper 1434, p. 133–161.

Williams, G.P., and Guy, H.P., 1973, Erosional and depositional aspects of Hurricane Camille in Virginia, 1969: U.S. Geological Survey Professional Paper 804, 80 p.

Wilson, R.C., 1989, Rainstorms, pore pressures, and debris flows; A theoretical framework, *in* Sadler, P.M., and Morton, D.M., eds., Landslides in a semi-arid environment: Publications of the Inland Geological Society, v. 2, p. 101–117.

☆U.S. GOVERNMENT PRINTING OFFICE:1998-673-441/23014